Integrating discovery-driven proteomics and selected reaction monitoring to develop a non-invasive assay for geoduck reproductive maturation

Emma B. Timmins-Schiffman[1], Grace A. Crandall[2], Brent Vadopalas[2], Michael E. Riffle[3], Brook L. Nunn[1], Steven B. Roberts[2,*]

[1] Department of Genome Sciences, University of Washington, Seattle, WA 98105

[2] School of Aquatic and Fishery Sciences, University of Washington, Seattle, WA 98105

[3] Department of Biochemistry, University of Washington, Seattle, WA 98105

* Corresponding author:

Steven B. Roberts, School of Aquatic and Fishery Sciences, University of Washington, 1122 NE Boat Street, Seattle WA 98105. email: sr320@uw.edu

Abstract

Geoduck clams (*Panopea generosa*) are an increasingly important fishery and aquaculture product along the eastern Pacific coast from Baja California, Mexico to Alaska. These long-lived clams are highly fecund, though sustainable hatchery production of genetically diverse larvae is hindered by the lack of sexual dimorphism, resulting in asynchronous spawning of broodstock, unequal sex ratios, and low numbers of breeders. Development of assays of gonad physiology could indicate sex and maturation stage, as well as be used to assess the status of natural populations. Proteomic profiles were determined for three reproductive maturation stages in both male and female clams using data dependent acquisition (DDA) of gonad proteins. Gonad proteomes became increasingly divergent between males and females as maturation progressed. The DDA data was used to develop targets analyzed with selected reaction monitoring (SRM) in gonad tissue as well as hemolymph. The SRM assay yielded a suite of indicator peptides that can be used as an efficient assay to determine geoduck gonad maturation status. Application of SRM in hemolymph samples demonstrates this procedure could effectively be used to assess reproductive status in marine mollusks in a non-lethal manner.

Key words: reproduction, gonad, geoduck, hemolymph, mollusk, proteomics, SRM, targeted proteomics

47 **Introduction**

48 Wild Pacific geoduck clams (*Panopea generosa*), like other suspension feeders, provide
49 vital ecosystem services as both primary consumers of phytoplankton and biodepositors.[1]
50 Additionally, commercial geoduck fisheries provide significant social benefits as the most
51 economically important clam fishery in North America.[2] Commercial farming of geoduck now
52 generates over 20 million dollars in annual sales and geoduck are among the most valuable
53 farmed shellfish on a per acre basis.[3] The rapid development of geoduck aquaculture close to
54 wild populations of conspecifics has raised concerns over farmed-wild interbreeding and the
55 subsequent loss of genetic diversity. To address these concerns, geoduck hatcheries are currently
56 encouraged to use large numbers of wild broodstock to maximize genetic diversity in farmed
57 geoducks. An ongoing impediment to fulfilling this conservation goal is the absence of nonlethal
58 identification methods for sex and maturation stage determination in broodstock. Geoducks are
59 not sexually dimorphic, thus sex is not accurately determined until spawning, which can be
60 induced through increase in temperature and microalgae ration. Further, at a given event, only a
61 few of the broodstock mature and spawn. Highly skewed sex ratios in some populations and the
62 inability to determine when to induce spawning based on maturation state present additional
63 challenges.

64 To date, only a few studies have investigated molecular or biochemical analyses to
65 identify sex or reproductive stages in marine invertebrates. For example, studies on vertebrate
66 steroids explored these organic molecules as an analyte for tracking mollusk reproduction
67 processes and stages.[4] There is suggestive evidence of steroidal metabolism and response in
68 mollusks, but these pathways remain poorly understood in terms of biochemical mechanism and
69 biological function.[5] Further research on gonad lipids [6], specific gene transcripts [7,8], and

70 RNA/DNA ratios [9] have clarified some of the physiology underlying molluscan sexual
71 maturation. A comprehensive study of the Pacific oyster gonadal gene expression across
72 reproductive stages further explained the molecular mechanisms at play [10]; however, none of
73 these studies translated physiological discovery into an applied assay.

74 Previous studies have demonstrated the promise of protein based assays for
75 characterization of reproductive status in bivalves. Arcos et al. [11] explored the use of enzyme-
76 linked immunoassay assays (ELISA) to quantify proteins associated with vitellogenesis to
77 determine oyster oocyte maturation. Although the two proteins targeted by Arcos et al. [11]
78 allowed distinction of males and females and differentiation of female reproductive stages, the
79 assay relies on a single physiological measure and cannot be adapted to a non-lethal assay. [4] The
80 complexity of molluscan reproductive maturation at the molecular level has been proven by
81 global profiling studies [10,12] that reveal possibilities for an informative assay that leverages the
82 involvement of diverse biochemical pathways.

83 Here, we apply mass spectrometry (MS)-based proteomics technology to provide a large-
84 scale, unbiased approach for examining relative abundances of all proteins present in gonad
85 tissue across several maturation stages of both female and male geoducks. Whole proteome
86 characterization via data dependent acquisition (DDA) provided basic information on
87 gametogenesis, gonad maturation, and informed peptide selection for the determination of sex
88 and maturation stage in subsequent downstream MS analyses. Selected peptides underwent
89 targeted proteomic analyses via selected reaction monitoring (SRM) to more accurately quantify
90 protein abundance. Together, these data provide fundamental insight into marine mollusk
91 reproductive biology and demonstrate effective non-invasive peptide quantification on
92 circulating hemolymph.

93

94 **Methods**

95 *Tissue Sampling*

96 Geoduck clams were collected in November 2014 from Nisqually Reach, Washington
97 (latitude:47 08.89, longitude:122 47.439 WGS84). Clams were collected at depths between 9 to
98 14 meters from a sandy substrate. Gonad tissue and hemolymph from geoduck clams at early-,
99 mid-, and late-stage gonad maturation, from both males and females, were characterized
100 histologically. Female reproductive maturation stages were categorized as follows: early-stage
101 (no secondary oocytes, or oocytes that measure ~5-15μ), mid-stage (secondary oocytes ~50-
102 70μ), and late-stage (secondary oocytes ~65-85μ). Male reproductive maturation stages were
103 characterized as follows: early-stage (mostly somatic cells and ~5% spermatid composition per
104 acinus), mid-stage (about equal parts somatic cells and reproductive tissue and ~50% spermatid
105 composition per acinus), and late-stage (very little somatic cells and ~75-90% spermatid
106 composition per acinus). Details of gonadal maturation classification and histological details
107 have been previously described.[13] Gonad tissue samples were taken from 3 early-stage females
108 (fG03, fG04, fG08), 3 mid-stage females (fG34, fG35, fG38), 3 late-stage females (fG51, fG69,
109 fG70), 3 early-stage males (mG02, mG07, mG09), 3 mid-stage males (mG41, mG42, mG46),
110 and 3 late-stage males (mG65, mG67, mG68) with identification codes corresponding to those
111 reported in Crandall et al.[13] Hemolymph tissue samples were taken from 3 early-stage females
112 (fG18, fG29, fG30), 2 mid-stage females (fG25, fG35), 3 late-stage females (fG51, fG69, fG70),
113 3 early-stage males (mG17, mG20, mG028), 2 mid-stage males (mG42, mG46), and 3 late-stage
114 males (mG65, mG67, mG68).

115

116 *Protein Preparation*

117 Gonad tissue from the eighteen geoduck clams was sonicated in lysis buffer (50 mM
118 NH_4HCO_3, 6 M urea). Gonad tissue protein homogenate content and hemolymph protein content
119 were quantified using Pierce BCA Protein Assay Kit (Thermo Fisher Scientific, Waltham, MA;
120 catalog #23225). Protein (100 µg - gonad samples, 50 µg - hemolymph) was evaporated to ~20
121 µl and resuspended in 100 µl of lysis buffer followed by sonication. Protein digestion for gonad
122 tissue samples and hemolymph followed the protocol outlined in Timmins-Schiffman et al.[14]
123 Briefly, each sample was incubated with 200 mM tris(2-carboxyethyl)phosphine buffered at pH
124 8.8 (1 hr, 37°C). Samples were alkylated with 200 mM iodoacetamide (IAM; 1hr, 20°C)
125 followed by an incubation (1 hr) with 200 mM dithiothreitol to absorb any remaining IAM. To
126 each sample, NH_4HCO_3 and HPLC grade methanol were added to dilute urea and to increase
127 solubilization of membrane proteins. Samples were digested overnight with trypsin at
128 37°C. Digested samples were evaporated and reconstituted in 5% acetonitrile (ACN) + 0.1%
129 trifluoroacetic acid (TFA) (100 µl) and pH was decreased to < 2. Desalting of the samples was
130 done using Macrospin columns (sample capacity 0.03-300 µg; The Nest Group, Southborough,
131 MA, USA) following the manufacturer's specifications. Dried peptides were reconstituted in
132 100 µl of 5% ACN + 0.1% formic acid.

133

134 *Global Proteome Analysis: Data-Dependent Acquisition (DDA) LC-MS/MS*

135 Data-dependent acquisition (DDA) was performed to examine gonad proteomic profiles
136 across samples (Figure 1). Liquid chromatography coupled with tandem mass spectrometry (LC-
137 MS/MS) was accomplished on a Q-Exactive-HF (Thermo) on technical triplicates for each
138 sample. The analytical column (20 cm long) was packed in-house with C18 beads (Dr. Maisch

139 GmbH HPLC, Germany, 0.3 µm) with a flow rate of 0.3 µl/min. Chromatography was
140 accomplished with an increasing ratio of solvent A (ACN + 0.1% formic acid): solvent B (water
141 + 0.1% formic acid). The solvent gradient consisted of: 0-1 minutes of 2-5% solvent A; 1-60
142 minutes 5-35% solvent A; 60-61 minutes 35-80% solvent A; 61-70 minutes 80% solvent A; 71-
143 90 minutes 80-2% solvent A. Quality control standards (Pierce Peptide Retention Time
144 Calibration mixture (PRTC) + bovine serum albumin peptides (BSA)) were analyzed throughout
145 the experiment to ensure consistency of peptide detection and elution times.
146

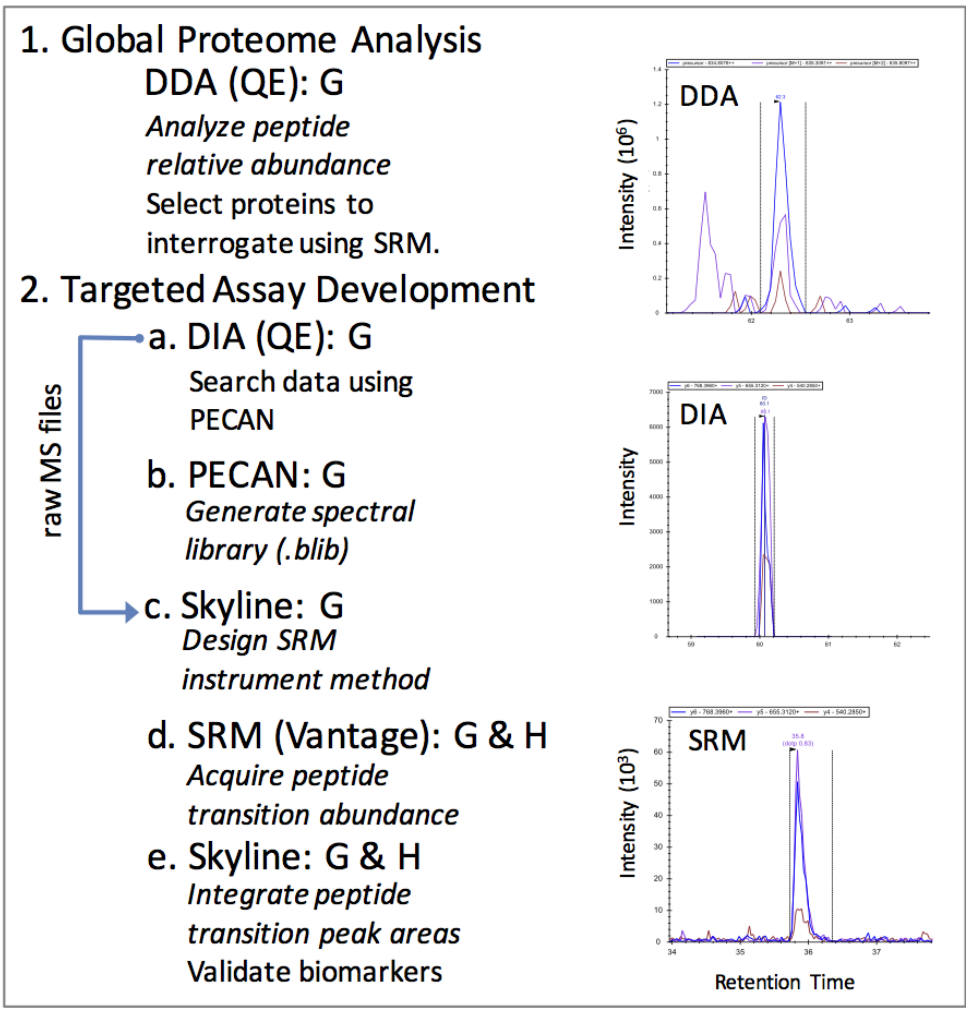

147

148 *Figure 1. Illustration of experimental setup and workflow for mass spectrometry data acquisition*

149 *and analysis. MS experimental workflow: 1. Data dependent acquisition (DDA) was performed*
150 *on the Q-Exactive-HF (QE) to assess the global proteomic differences in gonad (G) tissue*
151 *between sexes and maturation stages. 2. Targeted assay development followed the steps of (a)*
152 *data independent acquisition (DIA) on gonad tissue was also completed on the QE to create*
153 *spectral libraries for selected reaction monitoring (SRM) method development; (b & c) spectral*
154 *libraries were analyzed in PECAN using Skyline to select optimal transitions and design an*
155 *instrument method for SRM analyses; (d) SRM was completed on the TSQ Vantage for geoduck*
156 *peptide transitions in gonad and hemolymph (G & H); (e) Peptide transition detection and*
157 *quantification was performed in Skyline. The chromatograms of peptide KEEELIDYMVKQ*
158 *(from protein 130261_c0_seq1|m.17926) were collected using the 3 different MS approaches*
159 *(DDA, DIA, and SRM) from the same late-stage female. Black vertical lines indicate peak*
160 *integration boundaries, and colored peaks represent the different transitions (i.e. peptide*
161 *fragments) collected.*
162
163 *DDA protein identification and quantification*
164 Gonad peptides were identified and proteins inferred using a proteome derived from a *de*
165 *novo* assembled transcriptome of a male and female geoduck clam gonad tissue libraries (NCBI
166 Bioproject Accession #PRJNA316216) (Del Rio-Portilla et al., unpublished). Briefly, reads were
167 assembled using Trinity [15] and deduced protein sequences determined using the Transdecoder
168 algorithm within Trinity. Raw mass spectrometry data (PRIDE Accession #PXD003127) was
169 searched against the protein sequences using Comet v 2016.01 rev.2.[15,16] Parameters used with
170 Comet included concatenated decoy search, specifying trypsin as the cleaving enzyme, two
171 missed cleavages allowed, peptide mass tolerance of 20 ppm, cysteine modification of 57 Da

172 (from the IAM) and methionine modification of 15.999 Da (from oxidation) to find peptide
173 spectral matches (all parameters can be found in Supporting information 2). Protein inference
174 and match probability were found using the Trans-Proteomic Pipeline.[16,17] Data files were
175 combined and normalized spectral abundance factor (NSAF) [18] was calculated in Abacus [19] to
176 determine consistent protein inferences across replicates. Protein identifications were considered
177 true matches when the probability of the match was at least 0.8611 (corresponding to error rate,
178 which approximates FDR, of 0.01) and at least 2 independent spectra were associated with the
179 protein across all samples.

180 Non-metric multidimensional scaling analysis (NMDS) was used to determine the
181 similarity of technical replicates (Supporting Information 3) using the vegan package [20] in R v.
182 3.2.3[21]. NMDS was performed on log-transformed data using a Bray-Curtis dissimilarity
183 matrix. As technical replicates clustered closely together and showed less variability than
184 biological replicates (Supporting Information 3), NSAF was averaged across each sample
185 (n=18). [18] Proteomic differences between sexes and maturation stages were explored with two
186 methods: 1) NMDS and analysis of similarity (ANOSIM) were used to compare the entire
187 proteomic profiles in multivariate space and 2) Fisher's exact test was used to determine
188 significant differences at the individual protein level. NMDS was performed on NSAF data
189 followed by ANOSIM in the vegan package in R to determine the differences between sexes and
190 maturation stages. Differentially abundant proteins among the six conditions were identified
191 using [22]Fisher's exact test in Excel. Spectral counts were summed across technical replicates to
192 compare biological replicates. Nine comparisons were analyzed for differentially abundant
193 proteins: Early-stage male (EM) vs. early-stage female (EF); mid-stage male (MM) vs. mid-stage
194 female (MF); late-stage male (LM) vs. late-stage female (LF); EM vs. MM; EM vs. LM; MM vs.

195 LM; EF vs. MF; EF vs. LF; MF vs. LF. All p-values resulting from the test were multiplied by 9
196 as a Bonferroni correction for multiple comparisons. Proteins with a corrected p-value ≤ 0.05
197 were considered differentially abundant.
198
199 *Enrichment Analysis*
200 We used enrichment analysis to determine biological processes (represented by detected
201 proteins) predominant in each gonad sample. GO enrichment analysis was performed for each
202 maturation stage (for each sex) on 1) unique proteins and 2) all detected proteins. In both cases,
203 the entire detected proteome was used as the background. Enrichment analysis was also
204 performed on sets of differentially abundant proteins. Code used to perform enrichment analysis
205 is available in a corresponding GitHub repository (https://github.com/yeastrc/compgo-geoduck-
206 public) as is the underlying code for the end user web-interface
207 (http://yeastrc.org/compgo_geoduck/pages/goAnalysisForm.jsp).
208 Briefly, a p-value was calculated describing the enrichment of a GO term in a set of tested
209 proteins above what would be expected by chance, given the annotation of the geoduck gonad
210 proteome (3,627 proteins). A p-value cutoff of 0.01 was used to ascribe statistical significance to
211 GO terms representing biological process.
212 GO terms were first assigned directly to the geoduck gonad protein names resulting from
213 the *de novo*-assembled transcriptome. This was done by assigning GO terms associated with
214 Uniprot-KB Swiss-Prot BLASTp hits. A p-value representing the statistical significance of the
215 representation of a GO term in a set of proteins was calculated using the hypergeometric
216 distribution using the following formula:

$$P(I) = \frac{\binom{A}{I} * \binom{T-A}{B-I}}{\binom{T}{B}}$$

Where A = total number of proteins submitted that have a GO annotation, B = the total number of proteins in the background proteome annotated with the given GO term (or any of its descendants), I (intersection of A and B) = the total number of submitted proteins annotated with the given GO term (or any of its descendants), and T = the total number of annotated proteins in the proteome background.

Then, the p-value describing the chance of having an intersection of size I or larger by chance may be computed as:

P-value = $\sum_{i=I}^{\min(A,B)} P(i)$, where min (A,B) is the minimum of values A and B.

The p-value is then corrected for multiple hypothesis testing using the Bonferroni method by multiplying the p-value by the number of GO terms tested (setting resulting values over 1 to 1). The number of GO terms tested equals the number of GO terms found (and all ancestors) for the submitted set of proteins.

Complete directed acyclic graphs (DAG) that represent a subset of the whole GO DAG were generated to visualize enriched biological processes. These DAGs were then filtered by removing all childless terms that had an associated p-value $\geqslant$ 0.01. The resulting DAGs were then filtered using the same method, and this process repeated until no childless terms remained with a p-value above the cutoff. The final result is a filtered subset of the GO DAG that contains no leaf nodes with a p-value greater than the cutoff, but where a given term is guaranteed to have

236 all of its ancestor terms, even if those terms have a p-value greater than the cutoff. Having the
237 ancestor terms present is critical to visualization as they provide context for interpreting the
238 results. Proteins that contribute to specific enriched processes for all enrichment analyses are
239 included in Supporting Information 4 and visualizations of enrichments for full and unique
240 proteomes for each sex and stage are visualized in a single DAG for each sex and stage
241 (Supporting Information 3). Venn diagrams of enriched processes were produced in Venny [22].
242
243 *Targeted Assay Development: Selected Reaction Monitoring (SRM)*
244 A subset of proteins was chosen for development of a suite of targeted assays using
245 selected reaction monitoring (SRM) on the mass spectrometer. Based on the data dependent
246 acquisition, proteins that were detected in only one gonadal stage (early-stage males (EM), early-
247 stage females (EF), late-stage males (LM), or late-stage females (LF)) or were at considerably
248 higher abundance in one of these stages were screened for usable peptide transitions in SRM in
249 Skyline daily v. 3.5.1.9706 [23].
250 Data independent acquisition (DIA) was used to generate spectral libraries for biomarker
251 development in the gonad tissue (Figure 1). Equal amounts of isolated peptides from the three
252 biological replicates for EM, EF, LM, and LF used in the DDA experiment (described above)
253 were pooled in equal quantities for DIA on the Q-Exactive HF (Thermo). Each sample included
254 a spiked-in internal quality control peptide standard (375 fmol PRTC; Pierce). Sample injections
255 for all DIA experiments included protein (1 µg) plus PRTC (50 fmol) in a 2 µl injection. An
256 analytical column (27cm) packed with C18 beads (3 µm; Dr. Maisch) and a trap (3 cm) with C12
257 beads (3 µm; Dr. Maisch) were used for chromatography. Technical replicate DIA spectra were
258 collected in 4 m/z isolation width windows spanning 125 m/z ranges each [24] (400-525, 525-650,

259 650-775, 775-900). For each method, a gradient of 5-80% ACN over 90 minutes was applied for
260 peptide spectra acquisition. Raw data can be accessed via ProteomeXchange under identifier
261 PXD004921. MSConvert [25] was used to generate mzML files from the raw DIA files.

262 Peptide Centric Analysis was completed with the software program PECAN to generate
263 spectral libraries for targeted method development. [26] Input files included the list of peptides
264 generated for SRM (n=217), as described above, and the mzML files generated from the raw
265 DIA files. PECAN correlates a list of peptide sequences with the acquired DIA spectra to locate
266 the peptide-specific spectra within the acquired DIA dataset. A background proteome of the *in*
267 *silico* digested geoduck gonad proteome was used.

268 The PECAN output file (.blib) was imported into Skyline to select peptide transitions and
269 create MS methods that would target specific peptides and transitions. Peptide transitions are the
270 reproducible fragments of peptides that are generated during the MS2 scan. Peptides reliably
271 fragment in the same way in the mass spectrometer, therefore transitions are a robust and
272 consistent signal of a peptide's presence.[27] Peptide transitions were selected if peak morphology
273 was uniform and consistent across the MS2 scans for technical replicates. Peptides were selected
274 for targeted analysis if they had $\geq$ 3 good quality transitions and there were $\geq$ 2 peptides per
275 protein. A maximum of 4 transitions per peptide were selected for targeted analysis and no more
276 than 3 peptides per protein were selected. This transition list was divided between two method
277 files for the final SRM analyses to provide adequate dwell time on individual transitions to
278 accurately detect and measure all peptides desired.[28]

279 Selected reaction monitoring (SRM) was carried out on a Thermo Vantage for all
280 eighteen geoduck gonad samples used in the original DDA analysis. Samples were prepared as
281 described above for DIA (1 µg of protein per 3 µl injection). A new C18 trap (2 cm) and C18

282 analytical column (27.5 cm) were used and each sample was analyzed in triplicate across two
283 MS experiments to cover the entire peptide transition list (n=228, 217 of which yielded
284 quantifiable data). Raw data can be accessed in the PeptideAtlas under accession PASS00943.
285 Hemolymph from early-, mid-, and late-stage males and females was also assayed for
286 sex- and stage-specific biomarkers. An augmented SRM assay was used on the hemolymph that
287 included all the peptide transitions analyzed in the gonad with an additional 40 transitions from
288 five new proteins. These proteins were selected based on gonad proteome annotation to include
289 1) proteins that would likely be circulating in the hemolymph and 2) gonad proteins that had
290 homology with the mussel hemolymph proteome.[29] The additional peptides for SRM analysis of
291 hemolymph were from vitellogenin (2 proteins: cds.comp100108_c2_seq1|m.5995,
292 cds.comp144315_c0_seq1|m.50928), glycogen synthase (2 proteins:
293 cds.comp140343_c0_seq2|m.34696, cds.comp141785_c0_seq1|39776), and glycogenin-1
294 (cds.comp140645_c0_seq3|m.35608). PECAN generated spectral libraries, as described above,
295 and Skyline software selected hemolymph protein transitions to target during SRM analyses. For
296 the new hemolymph proteins, the minimum targets for peptides (≥3) and transitions (≥2) as
297 described for gonad SRM could not be met for every protein, but were still included in the
298 analysis. These transitions, and the previous gonad transitions (total of n = 254), were analyzed
299 across sixteen geoduck hemolymph samples in two technical replicates, as described above for
300 the gonad. Some of these peptides yielded no data in the hemolymph, resulting in a dataset of
301 171 peptide transitions that were reliably detected. Raw data can be accessed in PeptideAtlas
302 under accession PASS00942.
303 Acquired SRM data in gonad and hemolymph were analyzed in Skyline for peptide
304 transition quantification. Skyline documents that were used to analyze the monitored peptide

305 transitions can be found on Panorama for the gonad dataset and the hemolymph datasets
306 (panoramaweb.org/labkey/geoduckrepro.url). Accurate Peak detection was determined based on
307 consistency of retention time (verified by spiked in PRTC peptides and correlation with DIA
308 peptide retention times) and peak morphology.

309 All peptide transition peak intensities were exported from Skyline for automated peak
310 selection and peak integration analysis. PRTC internal standard transitions were monitored for
311 consistency across runs by calculating the coefficient of variation (CV) of transition peak area
312 across injections. Peak intensities for the geoduck peptide transitions were normalized by
313 dividing by the averaged intensities for the 6 PRTC peptide transitions that had the lowest CV in
314 the gonad data (CV < 13) and the 6 with the lowest CV in the hemolymph data (CV < 10).

315 NMDS and ANOSIM were performed on the PRTC-normalized SRM dataset as
316 described above for the DDA dataset, except data were log(x+1) transformed for the gonad SRM
317 dataset. An initial NMDS showed that technical replicates clustered together well and that
318 variation was lower within biological replicates compared to between replicates, therefore
319 technical replicate peak intensities were averaged for the rest of the analysis (Supporting
320 Information 3). ANOSIM was performed using grouping by sex and reproductive stage alone, as
321 well as by a combined sex-stage factor. Coefficients of variation were calculated for combined
322 technical replicates using the raster [30] package in R.

323 Eigenvector loadings were calculated for the gonad and hemolymph data using the vegan
324 package in R. For each dataset, the top 20 transitions with the combination of lowest p-value and
325 highest loading value for each MDS axis were selected as biomarkers. Heatmaps of the log-
326 normalized transition intensities for these biomarkers were made using pheatmap[31] in R,
327 clustering rows (peptide transitions) and columns (samples) using euclidean distance and the

328 average clustering method.

329

330 **Results**

331 *DDA Proteomics*

332 The mass spectrometry data (PRIDE Accession #PXD003127) interpreted with a species-
333 and tissue-specific transcriptome yielded 3,651 proteins inferred with high confidence across all
334 gonad tissue samples (total spectral count across all replicates > 1) (Supporting Information
335 4). Female and male gonad proteomic profiles were more similar in early-stage maturation, with
336 proteomes diverging as reproductive maturity advanced (Figure 2). Proteomic profiles were
337 significantly different between sexes ($R = 0.4167$, $p = 0.001$) and maturation stages ($R = 0.3494$,
338 $p = 0.002$).

339 Unique proteomic profiles include the set of proteins that were detected in a specified sex
340 or specific stage within sex in the DDA analysis. The female proteomic profile across all stages
341 contained 156 unique proteins whereas 144 proteins were unique to males. The number of
342 proteins unique to a specific maturation stage increased with maturity from 16 and 18 in early-
343 stage females and males, respectively, to 132 and 104 in late-stage females and males (Figure 3).
344 Enriched GO biological processes for the unique proteins and all detected proteins for each sex
345 and stage are summarized in Table 1. Only the most specific GO terms (i.e., farthest down on the
346 DAG) are listed; parent terms were frequently enriched as well and can be seen in the DAGs
347 (Supporting Information 3).

348

349

350

351 *Table 1. Enriched biological process GO terms for the unique proteins and all detected proteins*

352 *in the gonad for each sex and stage. If no GO terms are listed, no enriched processes were*

353 *identified*

Gonad Stage	Detected Proteome GO terms	Unique Proteome GO terms
Early-stage Female	Translation	
Mid-stage Female	Translation	
Late-stage Female	Macromolecule biosynthetic process	Homophilic cell adhesion via plasma membrane adhesion molecules
Early-stage Male	Translation; Small molecule metabolic process	
Mid-stage Male	Translation; Nucleoside metabolic process; Purine-containing compound metabolic process	
Late-stage Male	Translation; Microtubule-based process; ribonucleoside metabolic process; ribonucleoside triphosphate metabolic process	Microtubule-based process

354

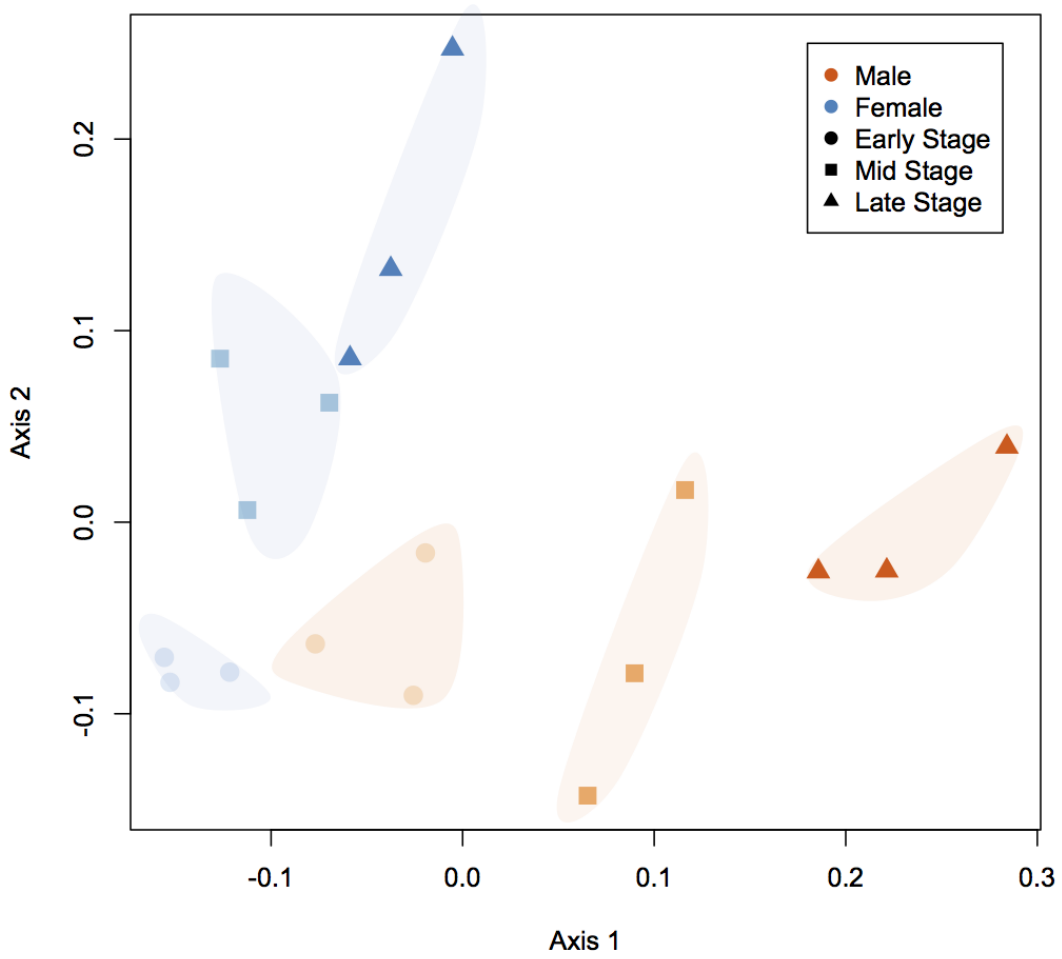

Figure 2. Non-metric multidimensional scaling plot (NMDS) of geoduck gonad whole proteomic profiles generated by data dependent acquisition. Gonad proteomes differ among clams by both sex (male = orange, female = blue) and stage (early-stage = circles, mid-stage = squares, late-stage = triangles; $p<0.05$).

Numerous proteins were differentially abundant in comparisons between reproductive stage and sex based on analysis with a Fisher's exact test with Bonferroni correction for multiple comparisons. The number of differentially abundant proteins within a stage and between sexes

364 increased from 102 between early-stage males and females to 1109 between late-stage males and
365 females (Figure 4, Supporting Information 4). Enrichment analysis revealed which processes
366 were over-represented in the sets of differentially abundant proteins, when compared to the entire
367 proteome (Figure 4 and Supporting Information 4).
368

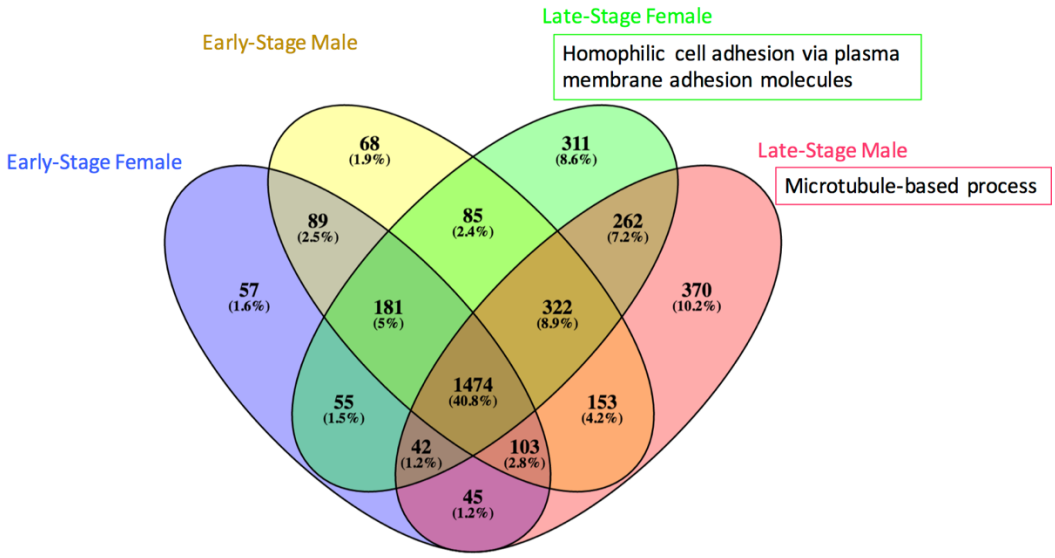

369

370 *Figure 3. Number of proteins detected in sex and stage specific proteomes for early-stage female*
371 *(blue), early-stage male (yellow), late-stage female (green), and late-stage male (red). Biological*
372 *processes enriched in the sex- and stage-specific proteomes compared to all proteins detected*
373 *across sexes and stages are listed for each proteome.*
374

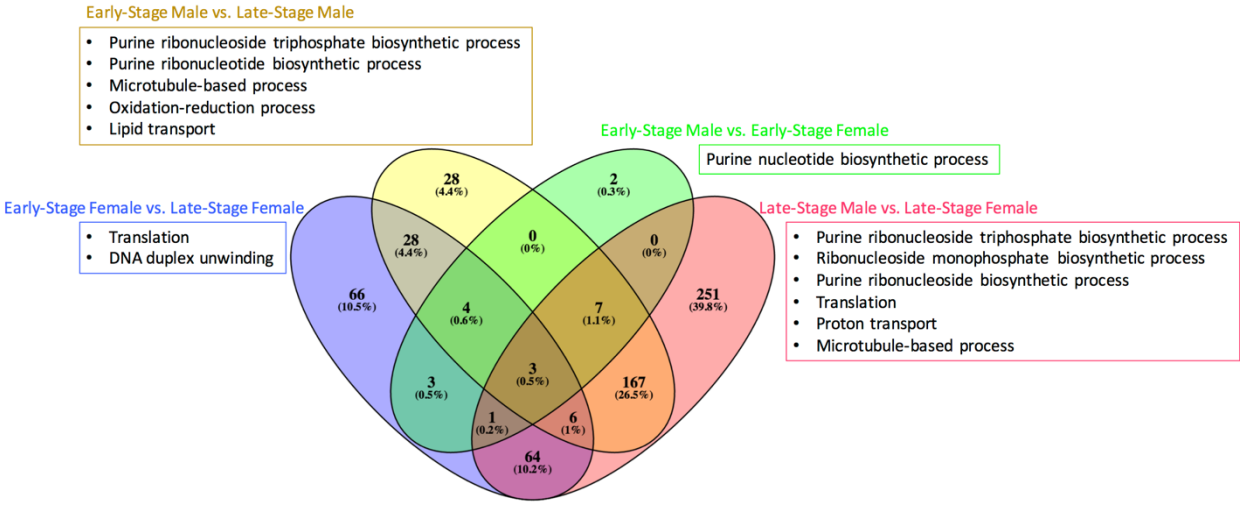

Figure 4. Number of differentially abundant proteins between geoduck sexes and stages based on comparisons between early-stage males and mid-stage males; early-stage males and late-stage males; early-stage females and mid-stage females; early-stage females and late-stage females. Biological processes enriched in the sets of differentially abundant proteins, compared to all proteins detected across sexes and stages, are listed for each proteome.

Targeted Assay Development: Selected Reaction Monitoring (SRM)

SRM was applied to create peptide assays that could resolve geoduck sex and maturation stages. Peptide transitions in the gonad (n=217) and hemolymph (n=171) derived from proteins detected in a single sex-maturation stage from one of the following: early-stage male (EM), early-stage female (EF), late-stage male (LM), and late-stage female (LF) proteomes were measured across 18 geoduck gonad samples and 16 hemolymph samples (Supporting Information 4). Many transitions had stable coefficients of variation across all biological replicates, although more an average of 3% of the peptide transitions had CVs > 100 across technical replicates for gonad samples and 10% were >100 for the hemolymph samples, indicating a need for assay optimization (Supporting Information 3).

392 In an ordination plot, the gonad SRM data resolved males and females better in late-stage
393 samples than the early- or mid-stage (Supporting Information 3). There was significant
394 separation based on gonad SRM data for sex (R = 0.2435, p=0.002), stage (R=0.1984, p=0.003),
395 and a combined sex-stage factor (R=0.3959, p=0.001). The hemolymph SRM data resolved the
396 late-stage female and mid-stage male groups from the rest of the geoduck (Supporting
397 Information 3). There was significant separation of the hemolymph proteomic profiles based on
398 stage (R=0.1772, p=0.048) and sex-stage (R=0.2749, p=0.028), but not by sex alone
399 (R=0.01786, p=0.37).
400 Peptide transitions that directed the observed spread of the geoduck sex-stage data along
401 Axis 1 and Axis 2 in the NMDS plots (determined by eigenvector analysis) were considered key
402 analytes for differentiating groups. These peptide transitions represent a starting point for
403 biomarker assay optimization. Peptides that drove the separation of the male maturation stages
404 along Axis 1 in the gonad NMDS plot (Supporting Information 4) are from a set of 7 proteins: IQ
405 domain-containing protein K (cds.comp133232_c0_seq1|m.21239), armadillo repeat-containing
406 protein (cds.comp140515_c2_deq1|m.35054), flap endonuclease
407 (cds.comp130260_c0_seq1|m.17926), dynein heavy chain (cds.comp144210_c0_seq2|m.50335),
408 spectrin alpha chain (cds.comp141647_c0_seq1|m.39026), and four uncharacterized proteins
409 (cds.comp135264_c2_seq1|m.24100, cds.comp133422_c0_seq1|m.21474,
410 cds.comp131654_c1_seq1|m.19394, cds.comp144596_c0_seq1|m.53297) (Figure 5). Proteins
411 that played a significant role in the separation of the female stages along Axis 2 for the gonad
412 data included centrosomal protein of 70 kDa (cds.comp133063_c0_seq1|m.21029), WD repeat-
413 containing protein on Y chromosome (cds.comp131715_c0_seq1|m.19472), tetratricopeptide
414 repeat protein 18 (cds.comp139151_c0_seq5|m.31757), and four uncharacterized proteins

(cds.comp131654_c1_seq1|m.19394, cds.comp139654_c0_seq1|m.32810, cds.comp135264_c2_seq1|m.24100, cds.comp140866_c0_seq1|m.36276). Analysis of the hemolymph SRM NMDS (Supporting Information 3) reveals that the main peptide drivers along Axis 1 (separating late-stage females and mid-stage males) were from six proteins: flap endonuclease (cds.comp130260_c0_seq1|m.17926), vitellogenin (cds.comp144315_c0_seq1|m.50928), spectrin alpha chain (cds.comp141647_c0_seq1|m.39026), vesicle-fusing ATPase (cds.comp144180_c0_seq1|m.39026), and two uncharacterized proteins (cds.comp138018_c0_seq1|m.29238, cds.comp133422_c0_seq1|m.21474) (Figure 6). A cluster analysis of the 40 transitions that were primary drivers of individual variation in the NMDS exposed a strong cluster of the females in the hemolymph data (Figure 6).

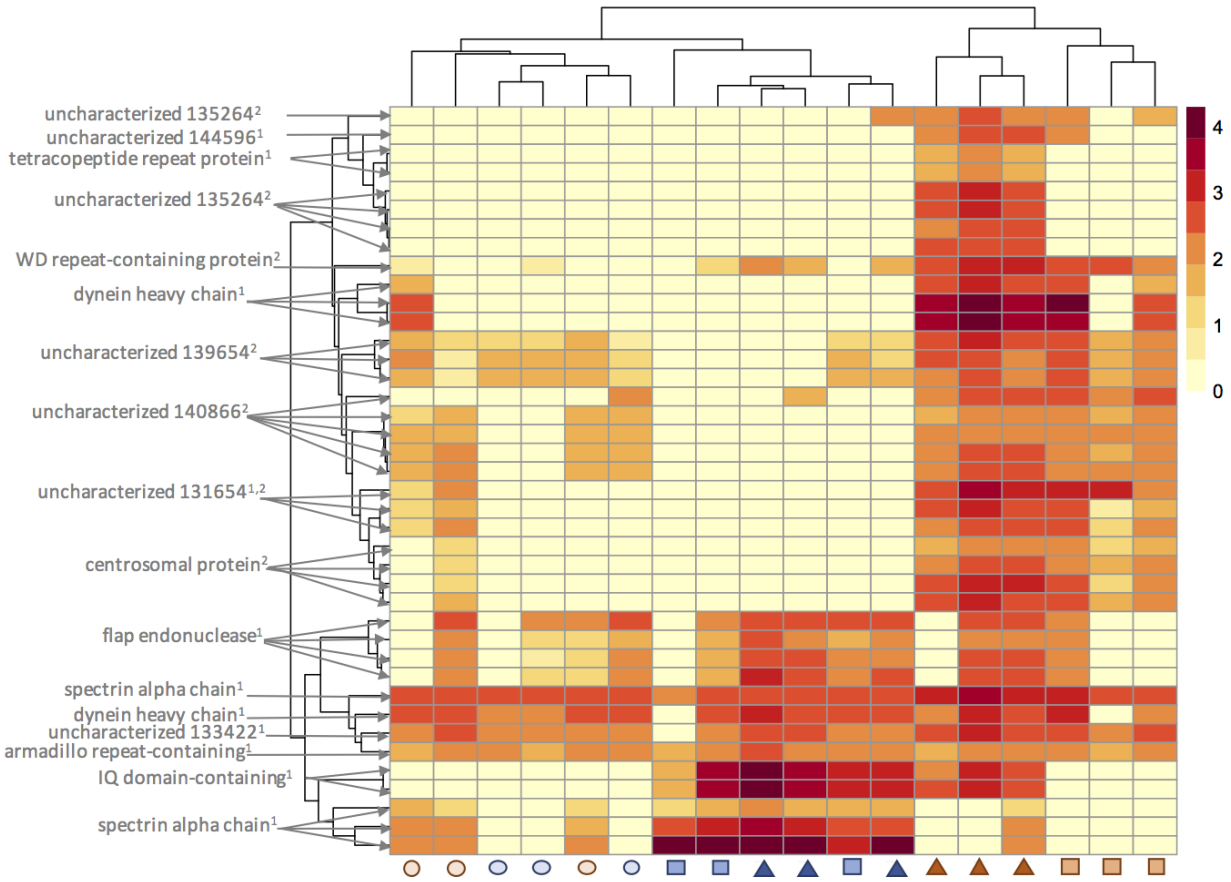

427 *Figure 5. Heatmap of log-normalized peptide transition intensities for 40 significant transitions*

428 *(based on NMDS analysis) across all samples (early-stage/circles, mid-stage/squares, and late-*

429 *stage/triangles males/orange and females/blue) gonad. Each row (peptide transition) is labeled*

430 *by its corresponding protein annotation in gray. Superscripts indicate for which NMDS axis a*

431 *transition is significant.*

432

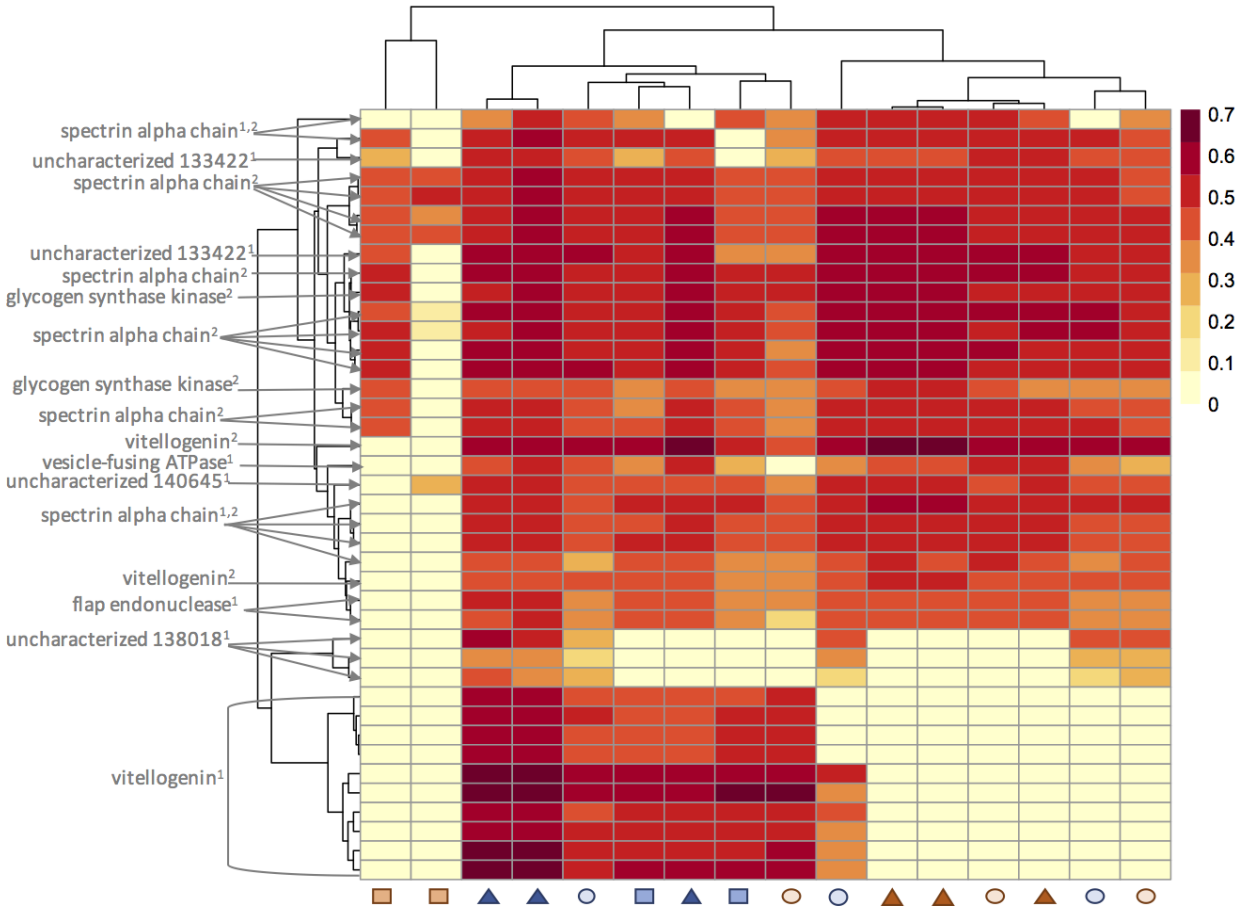

433

434 *Figure 6. Heatmap of log-normalized peptide transition intensities for 40 significant transitions*

435 *(based on NMDS analysis) across all samples (early-stage/circles, mid-stage/squares, and late-*

436 *stage/triangles males/orange and females/blue) hemolymph. Each row (peptide transition) is*

437 *labeled by its corresponding protein annotation in gray. Superscripts indicate for which NMDS*

438 *axis a transition is significant.*

439

440 **Discussion**

441 Proteomics has the capacity to uncover physiological processes underlying functional
442 phenotypic change, including the maturation of reproductive tissue. We have characterized the
443 geoduck clam gonad proteome throughout reproductive maturation for both males and females.
444 Our data dependent analysis (DDA) approach yielded 3,651 detected proteins across both sexes
445 and three maturation stages. This is a significant escalation in the understanding of proteomic
446 responses in maturation stages of marine mollusks. Based on the DDA data, 27 proteins (with a
447 corresponding 85 peptides) from early- and late-stage male and female clams were chosen for
448 selected reaction monitoring (SRM). Peptide transitions were detected from the selected peptides
449 as candidates for biomarker development in gonad (n=217) and in hemolymph (n=171).

450

451 *DDA*

452 There are clear proteomic profile differences in the geoduck gonad by both sex and
453 maturation stage and these differences reveal the biochemical pathways underlying tissue
454 specialization. More proteins were differentially abundant between early and late stages of
455 reproductive maturity, compared to early and mid-stages, for both males and females, reflecting
456 that, as maturation progresses, gonad tissue becomes more specialized, expressing a more
457 diverse array of regulatory and structural proteins. Gonad goes from undifferentiated connective
458 tissue to specialized structures that regulate gametogenesis and release of gametes. These
459 phenotypic changes required for reproductive maturity are evident with histology[13] and are
460 realized via changes at the protein level. For example, the zona pellucida (ZP) containing protein
461 (cds.comp134923_c0_seq3|m.23445) and vitellogenin (cds.comp144315_c0_seq1|m.50928)

462 were more abundant in the female gonad as geoduck matured. The zona pellucida surrounds
463 vertebrate oocytes and its invertebrate homolog is the vitelline envelope; the vitelline envelope is
464 likely the origin of the zona pellucida (ZP) containing protein and the site of sperm-oocyte
465 recognition and binding. Vitellogenin is an egg yolk protein precursor that is closely linked to
466 gametogenesis in bivalves. Increasing levels of vitellogenin are correlated with advancement in
467 reproductive maturation in oysters [32,33,34], clams [35], and mussels [36].

468 In females, enrichment analysis of unique proteins and all detected proteins revealed that
469 the early-stage gonad proteome was enriched in proteins involved in translation and cytoskeleton
470 structure and proteins associated with purine metabolism and translation were predominant
471 during the mid-stage. These protein-level changes likely represent alterations to cell morphology
472 and shifts in protein translation required to effect gonad structural and functional changes.

473 The late-stage female gonad proteome was enriched in proteins associated with cell
474 adhesion and translation/phosphorylation. Cell adhesion is an essential biological process in
475 maturing oocytes in vertebrates.[37,38] The strong cell adhesion signal in late-stage females was
476 driven in large part by the many cadherin and protocadherin proteins detected in a single female.
477 However, twelve protocadherins were detected at significantly higher abundance in more than a
478 single late-stage female when compared to early- and mid-stages. Further, the cell adhesion
479 proteins laminin, talin, and vinculin were less abundant in late-stage females compared to other
480 females. The shift from laminin, talin, and vinculin to cadherins during female gonad
481 development may signal a change in cell-cell interactions as oocytes form. There was also storng
482 Evidence for the importance of protein translation and phosphorylation. Proteins with homology
483 to several protein kinases were all detected solely in late-stage females. This surge in
484 phosphorylating proteins is likely a reflection of an increase in protein activation in the later

485 stages of gonad maturation.

486 Enriched processes in late-stage male geoduck gonad proteome including "kinesin
487 complex" and many microtubule-related functions reflect an increase in cell replication during
488 the last steps of sperm formation. Several proteins implicated in mitosis and meiosis were
489 detected at significantly increased abundance in late-stage males compared to early- and mid-
490 stage: dynein, intraflagellar transport protein, kinesin, and alpha and beta tubulin. All of these
491 proteins are instrumental in the cell division and replication and their importance at this
492 maturation stage suggests the presence of rapidly dividing cells. In mussels off the Atlantic coast
493 of Spain, meiotic division begins approximately four months before the onset of spawning, while
494 mitosis reconstructs the gonad during and after spawning.[39] These pieces of proteomic evidence
495 point towards increased cellular energy metabolism and cell division during the development of
496 mature, motile sperm.

497 Even with a highly specific protein identification database, the DDA method excludes
498 many important, relatively low abundance proteins from analysis.[40] The ten most abundant
499 proteins (as measured by total spectral count) for each sex-maturation stage accounted for 6-28%
500 of the total spectral counts across all proteins for a given sex-stage. Many of these proteins are
501 "housekeeping" proteins, such as actin and myosin, and their dominance in the peptide mixture
502 was likely masking many informative, low abundance peptides. Similarly, in zebrafish, highly
503 abundant vitellogenin (also highly abundant in the mid- and late-stage females in this study)
504 made it difficult to detect lower abundance proteins using DDA.[41]

505 The most abundant protein across all replicates likely plays an essential role in
506 reproductive maturation. The protein is glutamine gamma-glutamyltransferase, or
507 transglutaminase, and it has total spectral counts ranging from 259 to 1878 per MS analysis. The

508 annotation to this protein was only recently updated in Uniprot, so it was originally annotated as
509 "uncharacterized" in our BLAST search. Transglutaminase is typically associated with protein
510 cross-linking during wound healing in crustaceans[42] and bivalves[43] and also serves as a
511 biomarker for summer mortality in bivalves.[44] However, gene expression of this protein
512 transcript has also been linked to vitellogenesis in the shrimp *Panaeus monodon* where it is
513 hypothesized to mediate ovarian maturation via a hormone-receptor interaction[45]. The high
514 abundance of transglutaminase in our geoduck dataset suggests a key role in invertebrate
515 reproductive maturation. It is significantly more abundant in mid-stage males and females
516 compared to late- and early-stage stages as well as more abundant in late-stage females than
517 males, which is consistent with the shrimp study where its gene transcript was at highest
518 abundance in early vitellogenesis[45].
519
520 *SRM*
521 Selected reaction monitoring allows for the detection and absolute quantification of only
522 the most informative proteins' peptides to address a specific hypothesis. We leveraged the DDA
523 dataset to create informative SRM assays of geoduck sex and maturation stage in both gonad and
524 hemolymph. In the gonad tissue, we measured 217 peptide transitions that could differentiate
525 males and females as well as early and late maturation stages. Our assay is based on proteins that
526 are involved in calcium ion binding, phosphorylation, meiosis, DNA replication and repair, and
527 membrane structure. Additionally, seven of these informative proteins were unannotated. These
528 unknown proteins may represent taxon-specific reproductive proteins and warrant further
529 characterization. Reproductive proteins are some of the fastest-evolving, resulting in many
530 species-specific proteins.[46]

531 A subset of the peptide transitions (n=40) from these proteins were deemed highly
532 informative based on our analysis in gonad samples and would be good candidates for a more
533 streamlined SRM assay. These transitions correspond to eight annotated proteins and six
534 unannotated proteins. The annotated proteins are implicated in cytoskeleton structure (spectrin
535 alpha chain, dynein heavy chain), DNA replication and repair (centrosomal protein of 70 kDa,
536 flap endonuclease), and proteins that were identified by motifs and thus yield little functional
537 information (WD repeat-containing protein on Y chromosome, IQ domain containing protein K,
538 armadillo repeat-containing protein, and tetracopeptide repeat protein 18). The 40 transitions
539 were almost uniformly at higher abundance in late stage males and females, compared to earlier
540 reproductive stages.
541 The peptide-based assay developed from the evidence found in the gonad tissue was
542 applied to circulating hemolymph. We were able to collect data on 171 peptide transitions that
543 were derived from gonad tissue but detectable in the hemolymph, including all the transitions
544 that were added specifically to the hemolymph assay. Peptide transitions from 16 proteins were
545 reliably detected in both gonad and hemolymph, however, only three proteins had transitions that
546 were highly informative in both tissues: spectrin alpha chain, flap endonuclease, and an
547 uncharacterized protein. The inclusion of vitellogenin in our assay confirmed its presence in
548 geoduck hemolymph during later stages of reproductive maturity in females. Vitellogenin is an
549 informative proteomic biomarker for oyster and sea turtle female reproductive stage. [34, 47] In the
550 oyster study, vitellogenin fragments were among the most abundant proteins detected and were
551 particularly accumulated at greater abundances in oocytes associated with low production of
552 larvae.[34] In this case, it was hypothesized that greater accumulation of vitellogenin fragments in
553 the poor versus high quality oyster oocytes was indicative of the enzymatic breakdown of the

554 protein during oocyte ageing.[34]

555 The full suite of peptide transitions was not detected in hemolymph, likely due to
556 physiological differences between the tissues in which the assay was designed (gonad) and
557 applied (hemolymph). Biomarkers of tissue-specific changes can be difficult to detect in
558 circulating fluid since hemolymph is not the primary site of physiological change. Proteins and
559 their peptide fragments can yield physiologically relevant assays, even for organ-specific
560 changes [48], but may not be detectable due to different fragmentation patterns or delay in
561 abundance changes between the site of physiological change and the hemolymph or blood. In
562 geoduck hemolymph, 98 transitions were detected in the gonad but not in the hemolymph, but
563 119 transitions were detected in both tissues. Flap endonuclease and an uncharacterized protein,
564 detected in both tissues, were informative for late-stage female identification in the hemolymph
565 assay with flap endonuclease also an informative biomarker in gonad (Figures 5 & 6). The
566 hemolymph results emphasize both the flexibility and limitations of a peptide-based SRM assay
567 when designed for measurement of physiological change in a specific organ or tissue.

568 Through characterization of the geoduck gonad proteome and development of targeted
569 peptide-based assays for reproductive maturity, we not only exponentially increased genomic
570 resources available for this species, but we also provide an effective approach for non-lethal
571 detection of sex and maturation stage in this species. The gonad peptide transitions could be
572 optimized to a set of 40 transitions that would accurately predict a) geoduck sex and b)
573 reproductive maturation status. In the hemolymph, 40 peptide transitions can accurately
574 differentiate late-stage female and mid-stage male geoduck from others. Together these
575 molecular tools can directly address the geoduck production problem of asynchronous spawning
576 due to different maturation stages and unknown sexes.

Acknowledgements

This work was supported and funded by a grant from the University of Washington Royalty Research Fund (to SR), a Training Grant from the National Institutes of Health (to ETS) (T32 HG00035), and the University of Washington's Proteomics Resource (UWPR95794). We would like to thank Jimmy Eng and Priska von Haller for their help in data acquisition and analysis; Sonia Ting, Jarrett Egertson, Lindsay Pino, Yuval Boss, Brian Searle, and Nick Shulman for assistance with data analysis; the Genome Sciences Information and Technology group for their technical support; and Michael MacCoss for providing support and space to complete the work. ETS and BLN would like to thank IJE and TAN for their ongoing inspiration.

Supporting Information.

S-1 Cover page for Supporting Information.

S-2 Parameter file used in Comet searches for the DDA data

S-3 Plots demonstrating technical replication for DDA and SRM, and DAGs for enrichment analysis.

S-4 The first tab of the workbook contains all identified proteins from the DDA experiment with Uniprot annotations (e-value cut-off of 1E-10), total spectral counts for each technical replicate, calculated normalized spectral abundance factor (NSAF) for combined technical replicates, and indication of significantly differentially abundant proteins by pairwise comparison. Columns containing spectral count data have headers “SpC” preceded by the biological replicate number, sex, maturation stage, and technical replicate (for example, “EF3.1 SpC” is technical replicate 1

600 from early-stage female 3). Notation for NSAF is similar to notation for SpC. The 9 columns in
601 the sheet have headers such as "EFvLF" (comparison between early- and late-stage females)
602 have asterisks in the cells that correspond to proteins that were differentially abundant for each
603 given comparison. The last two columns ("NMDS Gonad" and "NMDS Hemolymph") have
604 asterisks in cells that correspond to the proteins with peptide transitions that contribute
605 significantly to the SRM NMDS plot distributions. The second tab contains GO biological
606 processes enriched in proteins that were differentially abundant between stages within a sex (e.g.
607 early- vs. mid-stage female) or between sexes within a stage (e.g LF vs. LM). Only the most
608 specific GO terms in the GO hierarchy are listed. No terms are listed when a comparison was not
609 made. The third through sixth tabs contain raw Skyline output (in the tab "Skyline output") and
610 peak intensities normalized by PRTC peptide abundance ("Normalized Intensities") for the
611 gonad and hemolymph SRM data.
612

613 **References**

614 (1) Newell, R. I. Ecosystem influences of natural and cultivated populations of suspension-
615 feeding bivalve mollusks: A review. *J. Shellfish Res.* **2004**, *23* (1), 51–62.
616 (2) Hoffmann, A.; Bradbury, A.; Goodwin, C. L. Modeling geoduck, Panopea abrupta (Conrad,
617 1849) population dynamics. I. Growth. *J. Shellfish Res.* **2000**, *19* (1), 57–62.
618 (3) Northern Economics, I. *The Economic Impact of Shellfish Aquaculture in Washington,*
619 *Oregon and California. Prepared for Pacific Shellfish Institute*; 2013.
620 (4) Scott, A. P. Do mollusks use vertebrate sex steroids as reproductive hormones? II. Critical
621 review of the evidence that steroids have biological effects. *Steroids* **2013**, *78* (2), 268–281.
622 (5) Fernandes, D.; Denise, F.; Barbara, L.; Cinta, P. Biosynthesis and metabolism of steroids in

623 molluscs. *J. Steroid Biochem. Mol. Biol.* **2011**, *127* (3-5), 189–195.

624 (6) Palacios, E.; Racotta, I. S.; Arjona, O.; Marty, Y.; Le Coz, J. R.; Moal, J.; Samain, J. F.
625 Lipid composition of the pacific lion-paw scallop, Nodipecten subnodosus, in relation to
626 gametogenesis. *Aquaculture* **2007**, *266* (1-4), 266–273.

627 (7) Anantharaman, S.; Craft, J. A. Annual variation in the levels of transcripts of sex-specific
628 genes in the mantle of the common mussel, Mytilus edulis. *PLoS One* **2012**, *7* (11), e50861.

629 (8) Ciocan, C. M.; Cubero-Leon, E.; Minier, C.; Rotchell, J. M. Identification of reproduction-
630 specific genes associated with maturation and estrogen exposure in a marine bivalve Mytilus
631 edulis. *PLoS One* **2011**, *6* (7), e22326.

632 (9) Li, Q.; Qi, L.; Makoto, O.; Katsuyoshi, M. Seasonal biochemical variations in Pacific oyster
633 gonadal tissue during sexual maturation. *Fish. Sci.* **2000**, *66* (3), 502–508.

634 (10) Dheilly, N. M.; Lelong, C.; Huvet, A.; Kellner, K.; Dubos, M.-P.; Riviere, G.; Boudry,
635 P.; Favrel, P. Gametogenesis in the Pacific oyster Crassostrea gigas: a microarrays-based
636 analysis identifies sex and stage specific genes. *PLoS One* **2012**, *7* (5), e36353.

637 (11) Arcos, F. G.; Ibarra, A. M.; del Carmen Rodríguez-Jaramillo, M.; García-Latorre, E. A.;
638 Celia, V.-B. Quantification of vitellin/vitellogenin-like proteins in the oysterCrassostrea
639 corteziensis(Hertlein 1951) as a tool to predict the degree of gonad maturity. *Aquac. Res.*
640 **2009**, *40* (6), 644–655.

641 (12) Li, Y.; Siddiqui, G.; Wikfors, G. H. Non-lethal determination of sex and reproductive
642 condition of Eastern oysters Crassostrea virginica Gmelin using protein profiles of
643 hemolymph by Proteinchip® and SELDI-TOF-MS technology. *Aquaculture* **2010**, *309* (1–
644 4), 258–264.

645 (13) Crandall, G.; Roberts, S. Reproductive Maturation in Geoduck clams (Panopea generosa)

646 https://figshare.com/articles/Reproductive_Maturation_in_Geoduck_clams_Panopea_genero
647 sa_/3205975/1.
648 (14) Timmins-Schiffman, E.; Nunn, B. L.; Goodlett, D. R.; Roberts, S. B. Shotgun proteomics
649 as a viable approach for biological discovery in the Pacific oyster. *Conserv Physiol* **2013**, *1*
650 (1), cot009.
651 (15) Grabherr, M. G.; Haas, B. J.; Yassour, M.; Levin, J. Z.; Thompson, D. A.; Amit, I.;
652 Adiconis, X.; Fan, L.; Raychowdhury, R.; Zeng, Q.; et al. *Full-length transcriptome*
653 *assembly from RNA-seq data without a reference genome*; 2011.
654 (16) Pedrioli, P. G. A. Trans-Proteomic Pipeline: A Pipeline for Proteomic Analysis. In
655 *Methods in Molecular Biology*; 2009; pp 213–238.
656 (17) Deutsch, E. W.; Mendoza, L.; Shteynberg, D.; Slagel, J.; Sun, Z.; Moritz, R. L. Trans-
657 Proteomic Pipeline, a standardized data processing pipeline for large-scale reproducible
658 proteomics informatics. *Proteomics Clin. Appl.* **2015**, *9* (7-8), 745–754.
659 (18) Florens, L.; Carozza, M. J.; Swanson, S. K.; Fournier, M.; Coleman, M. K.; Workman, J.
660 L.; Washburn, M. P. Analyzing chromatin remodeling complexes using shotgun proteomics
661 and normalized spectral abundance factors. *Methods* **2006**, *40* (4), 303–311.
662 (19) Damien Fermin, Vekatesha Basrur, Anastasia K. Yocum, and Alexey I. Nesvizhskii.
663 Abacus: A computational tool for extracting and pre-processing spectral count data for
664 label-free quantitative proteomic analysis. *Proteomics* **2011**, *11* (7), 1340–1345.
665 (20) Oksanen, J.; Guillaume Blanchet, F.; Friendly, M.; Kindt, R.; Legendre, P.; McGlinn, D.;
666 Minchin, P. R.; O'Hara, R. B.; Simpson, G. L.; Solymos, P.; et al. *vegan: Community*
667 *Ecology Package*; 2016.
668 (21) R Core Team. *R: A language and environment for statistical computing*; R Foundation

669 for Statistical Computing, Vienna, Austria, 2015.
670 (22) Choi, H.; Fermin, D.; Nesvizhskii, A. I. Significance analysis of spectral count data in
671 label-free shotgun proteomics. *Mol. Cell. Proteomics* **2008**, *7* (12), 2373–2385.
672 (22) Oliveros, J. C. *Venny. An interactive tool for comparing lists with Venn's diagrams*;
673 2007-2015.
674 (23) MacLean, B.; Tomazela, D. M.; Shulman, N.; Chambers, M.; Finney, G. L.; Frewen, B.;
675 Kern, R.; Tabb, D. L.; Liebler, D. C.; MacCoss, M. J. Skyline: an open source document
676 editor for creating and analyzing targeted proteomics experiments. *Bioinformatics* **2010**, *26*
677 (7), 966–968.
678 (24) Panchaud, A.; Scherl, A.; Shaffer, S. A.; von Haller, P. D.; Kulasekara, H. D.; Miller, S.
679 I.; Goodlett, D. R. Precursor acquisition independent from ion count: how to dive deeper
680 into the proteomics ocean. *Anal. Chem.* **2009**, *81* (15), 6481–6488.
681 (25) Chambers, M. C.; Maclean, B.; Burke, R.; Amodei, D.; Ruderman, D. L.; Neumann, S.;
682 Gatto, L.; Fischer, B.; Pratt, B.; Egertson, J.; et al. A cross-platform toolkit for mass
683 spectrometry and proteomics. *Nat. Biotechnol.* **2012**, *30* (10), 918–920.
684 (26) Ting, Y. S.; Egertson, J. D.; Payne, S. H.; Kim, S.; MacLean, B.; Käll, L.; Aebersold, R.;
685 Smith, R. D.; Noble, W. S.; MacCoss, M. J. Peptide-Centric Proteome Analysis: An
686 Alternative Strategy for the Analysis of Tandem Mass Spectrometry Data. *Mol. Cell.*
687 *Proteomics* **2015**, *14* (9), 2301–2307.
688 (27) Wolf-Yadlin, A.; Hautaniemi, S.; Lauffenburger, D. A.; White, F. M. Multiple reaction
689 monitoring for robust quantitative proteomic analysis of cellular signaling networks. *Proc.*
690 *Natl. Acad. Sci. U. S. A.* **2007**, *104* (14), 5860–5865.
691 (28) Picotti, P.; Aebersold, R. Selected reaction monitoring-based proteomics: workflows,

692 potential, pitfalls and future directions. *Nat. Methods* **2012**, *9* (6), 555–566.
693 (29) Moreira, R.; Pereiro, P.; Canchaya, C.; Posada, D.; Figueras, A.; Novoa, B. RNA-Seq in
694 Mytilus galloprovincialis: comparative transcriptomics and expression profiles among
695 different tissues. *BMC Genomics* **2015**, *16* (1), 728.
696 (30) Hijmans, R. J. Geographic Data Analysis and Modeling [R package raster version 2.5-8].
697 (31) Kolde, R. *pheatmap: Pretty Heatmaps*; 2015.
698 (32) Matsumoto, T.; Nakamura, A. M.; Mori, K.; Kayano, T. Molecular characterization of a
699 cDNA encoding putative vitellogenin from the Pacific oyster Crassostrea gigas. *Zoolog. Sci.*
700 **2003**, *20* (1), 37–42.
701 (33) Arcos, F. G.; Ibarra, A. M.; Rodríguez-Jaramillo, M. del C.; García-Latorre, E. A.;
702 Vazquez-Boucard, C. Quantification of vitellin/vitellogenin-like proteins in the oyster
703 Crassostrea corteziensis (Hertlein 1951) as a tool to predict the degree of gonad maturity.
704 *Aquac. Res.* **2009**, *40* (6), 644–655.
705 (34) Corporeau, C.; Vanderplancke, G.; Boulais, M.; Suquet, M.; Quéré, C.; Boudry, P.;
706 Huvet, A.; Madec, S. Proteomic identification of quality factors for oocytes in the Pacific
707 oyster Crassostrea gigas. *J. Proteomics* **2012**, *75* (18), 5554–5563.
708 (35) Blaise, C.; Gagné, F.; Pellerin, J.; Hansen, P. D. Determination of vitellogenin-like
709 properties inMya arenaria hemolymph (Saguenay Fjord, Canada): A potential biomarker for
710 endocrine disruption. *Environ. Toxicol.* **1999**, *14* (5), 455–465.
711 (36) Won, S.-J.; Novillo, A.; Custodia, N.; Rie, M. T.; Fitzgerald, K.; Osada, M.; Callard, I. P.
712 The Freshwater Mussel (Elliptio complanata) as a Sentinel Species: Vitellogenin and Steroid
713 Receptors. *Integr. Comp. Biol.* **2005**, *45* (1), 72–80.
714 (37) Fusi, F. M.; Vignali, M.; Busacca, M.; Bronson, R. A. Evidence for the presence of an

715 integrin cell adhesion receptor on the oolemma of unfertilized human oocytes. *Mol. Reprod.*
716 *Dev.* **1992**, *31* (3), 215–222.
717 (38) Campbell, S.; Swann, H. R.; Seif, M. W.; Kimber, S. J.; Aplin, J. D. Integrins and
718 adhesion mlecules: Cell adhesion molecules on the oocyte and preimplantation human
719 embryo. *Hum. Reprod.* **1995**, *10* (6), 1571–1578.
720 (39) Suárez, M. P.; Alvarez, C.; Molist, P.; Juan, F. S. PARTICULAR ASPECTS OF
721 GONADAL CYCLE AND SEASONAL DISTRIBUTION OF GAMETOGENIC STAGES
722 OF MYTILUS GALLOPROVINCIALIS CULTURED IN THE ESTUARY OF VIGO. *J.*
723 *Shellfish Res.* **2005**, *24* (2), 531–540.
724 (40) Pedersen, S. K.; Harry, J. L.; Sebastian, L.; Baker, J.; Traini, M. D.; McCarthy, J. T.;
725 Manoharan, A.; Wilkins, M. R.; Gooley, A. A.; Righetti, P. G.; et al. Unseen proteome:
726 mining below the tip of the iceberg to find low abundance and membrane proteins. *J.*
727 *Proteome Res.* **2003**, *2* (3), 303–311.
728 (41) Groh, K. J.; Nesatyy, V. J.; Segner, H.; Eggen, R. I. L.; Suter, M. J.-F. Global proteomics
729 analysis of testis and ovary in adult zebrafish (Danio rerio). *Fish Physiol. Biochem.* **2011**, *37*
730 (3), 619–647.
731 (42) Martin, G. G.; Jo Ellen Hose; Chong, C.; Hoodbhoy, T.; McKrell, N. Localization and
732 roles of coagulogen and transglutaminase in hemolymph coagulation in decapod
733 crustaceans. *Comparative Biochemistry and Physiology Part B: Comparative Biochemistry*
734 **1991**, *100* (3), 517–522.
735 (43) Nozawa, H.; Mori, T.; Kimura, M.; Seki, N. Characterization of a transglutaminase from
736 scallop hemocyte and identification of its intracellular substrates. *Comp. Biochem. Physiol.*
737 *B Biochem. Mol. Biol.* **2005**, *140* (3), 395–402.

738 (44) Chaney, M. L.; Gracey, A. Y. Mass mortality in Pacific oysters is associated with a
739 specific gene expression signature. *Mol. Ecol.* **2011**, *20* (14), 2942–2954.
740 (45) Sathapondecha, P.; Treerattrakool, S.; Panyim, S.; Udomkit, A. Potential roles of
741 transglutaminase and thioredoxin in the release of gonad-stimulating factor in Penaeus
742 monodon: implication from differential expression in the brain during ovarian maturation
743 cycle. *Mar. Genomics* **2011**, *4* (4), 279–285.
744 (46) Swanson, W. J.; Vacquier, V. D. The rapid evolution of reproductive proteins. *Nat. Rev.*
745 *Genet.* **2002**, *3* (2), 137–144.
746 (47) Plumel, M. I.; Wasselin, T.; Plot, V.; Strub, J.-M.; Van Dorsselaer, A.; Carapito, C.;
747 Georges, J.-Y.; Bertile, F. Mass spectrometry-based sequencing and SRM-based
748 quantitation of two novel vitellogenin isoforms in the leatherback sea turtle (Dermochelys
749 coriacea). *J. Proteome Res.* **2013**, *12* (9), 4122–4135.
750 (48) Klee, E. W.; Bondar, O. P.; Goodmanson, M. K.; Dyer, R. B.; Erdogan, S.; Bergstralh, E.
751 J.; Bergen, H. R., 3rd; Sebo, T. J.; Klee, G. G. Candidate serum biomarkers for prostate
752 adenocarcinoma identified by mRNA differences in prostate tissue and verified with protein
753 measurements in tissue and blood. *Clin. Chem.* **2012**, *58* (3), 599–609.

754